Revista de Metalurgia
July–September 2018, 54 (3), e122
ISSN-L: 0034-8570
https://doi.org/10.3989/revmetalm.122

Influence of an ERNiCrMo-3 root pass on the properties of cast iron weld joints

Manuel Pascual-Guillamón[a], Javier Cárcel-Carrasco[a,✉], Miguel Á. Pérez-Puig[a], Fidel Salas-Vicente[a]

[a]ITM, Universitat Politècnica de València, Camino de Vera, s/n. 46022 Valencia, España
✉Corresponding author: fracarc1@csa.upv.es

Submitted: 11 April 2017; Accepted: 17 December 2017; Available On-line: 26 July 2018

ABSTRACT: This article studies the effect of an ERNiCrMo-3 GTAW root pass on the microstructure and mechanical properties of a nodular cast iron joint when the cover passes are made using the SMAW technique and with Ni electrodes. To have a better understanding of the results, they are compared to the characteristics of a full Ni SMAW weld. This was done before and after an annealing at 900 °C in order to evaluate the influence and possible benefits of this heat treatment. The results show that the presence of a GTAW ERNiCrMo-3 root pass, despite improving penetration, leads to a loss of mechanical properties due to the presence of hard phases in the root pass that even an annealing is not able to eliminate.

KEYWORDS: Cast iron joint; Heat treatment; Mechanical properties; SMAW technique

Citation/Citar como: Pascual-Guillamón, M.; Cárcel-Carrasco, J.; Pérez-Puig, M.A.; Salas-Vicente, F. (2018). "Influence of an ERNiCrMo-3 root pass on the properties of cast iron weld joints". *Rev. Metal.* 54(3): e122. https://doi.org/10.3989/revmetalm.122

RESUMEN: *Influencia de la soldadura de raíz con ERNiCrMo-3 en las propiedades de las uniones soldadas de fundición nodular*. Este artículo estudia el efecto de la soldadura de raíz (GTAW) con ERNiCrMo-3 sobre la microestructura y propiedades mecánicas de una unión de fundición nodular cuando las pasadas de la cubierta se realizan con la técnica SMAW con electrodos de Ni. Para tener una mejor comprensión de los resultados, se comparan con las características de una soldadura completa de Ni SMAW. Esto se hizo antes y después de un recocido a 900 °C con el fin de evaluar las influencias y los posibles beneficios de este tratamiento térmico. Los resultados muestran que la presencia de una soldadura de raíz de GTAW ERNiCrMo-3, a pesar de la mejora de la penetración, conduce a una pérdida de propiedades mecánicas en la soldadura de raíz que, incluso con un recocido, no es posible eliminar.

PALABRAS CLAVE: GTAW; Propiedades mecánicas; Tratamiento térmico; Técnica SMAW; Uniones de fundición nodular

ORCID ID: Manuel Pascual-Guillamón (https://orcid.org/0000-0003-0216-5119); Javier Cárcel-Carrasco (https://orcid.org/0000-0003-2776-533X); Miguel Ángel Pérez-Puig (https://orcid.org/0000-0001-9343-9888); Fidel Salas-Vicente (https://orcid.org/0000-0003-0834-4425)

1. INTRODUCCIÓN

Graphite cast irons are basically alloys of iron, carbon –mainly with percentages between 2 and 4%- and silicon, which favours the formation of graphite instead of iron carbides.

The two most common graphite cast irons are grey and ductile iron. The difference between them is in the graphite formation. Gray iron is characterized by a random flake graphite pattern in a silicon-iron matrix, while in ductile iron the addition of magnesium or cerium to the alloy just before casting causes the graphite to form small spheroids rather than flakes. The discontinuities created by these nodular graphite formations are associated with a much better mechanical properties due to the fact that they do not act as stress concentrators or "internal notches" as graphite flakes do. That is why ductile iron -which is also referred to as "nodular iron"- combines the mechanical strength, toughness, and ductility of steel with the moldability (property of being moldable) of grey iron.

The high carbon content of these alloys makes them difficult to weld due to the formation of martensite and brittle iron carbides during cooling of the joined areas (Castolin, 1993; Arabi *et al.*, 2014). Due to this, welding on cast iron generally involves repair operations and not joining casting elements between them, although this last operation can be performed following some precautions (Cembrero and Pascual, 1999). These precautions are mainly oriented to the selection of the filler metal (Huke and Udin, 1953; El-Banna, 1999; Kiser *et al.*, 2005) and the reduction of the cooling rate of the weld in order to reduce martensitic transformations and carbide precipitations, which would with ease lead to the cracking of the joint. Geometry is also a main factor in the welding of cast iron due to its contribution to the rate of heat dissipation, but the welder has usually little control over it as it is something imposed.

Four types of filler metals are usually used: cast iron, copper base alloys, nickel base alloys and mild steel electrodes (El-Banna, 1999). Cast iron alloys are used for repairing tasks. While Cu alloys can provide sometimes good results due to its gammagen effect that minimizes the formation of brittle structures during weld cooling, Ni alloys are the ones more frequently selected when the mechanical characteristics of the joints are a principal parameter due the ductility they provide (Pease, 1960; El-Banna *et al.*, 2000; Pascual *et al.*, 2008). Mild steel electrodes produce joints with a reduced level of ductility and should be used only for small repairs. Austenitic steels have also been used, but cracking at the heat affected zone becomes an issue (Pouranvari, 2010).

Despite having selected the appropriate filler alloy, the heating and subsequent cooling of the material can produce brittle microstructures and, consequently, a faulty joint. The most useful techniques to reduce the cooling rate and avoid the formation of the aforementioned structures are, perhaps, to control the heat input and to preheat the casting in the range of 300–600 °C, although even less temperature could be enough (Pease, 1960; Martínez and Sikora, 1995). Nevertheless, although these precautions can reduce the amount of fragile structures along the heat affected zone (HAZ), a post-weld heat treatment is many times mandatory. If a moderate stress relief and softening is desired, heating to near 500 °C and slow air cooling are enough. Transformation of martensite to austenite, which will form a soft ferritic-pearlitic microstructure after a slow cooling can be achieved annealing the cast iron at 900 °C.

Besides having a relatively soft metallographic structure it's essential to assure a good penetration, mainly at the root of butt welds like the ones studied in this report. In order to obtain that good penetration and a high quality weld the Gas Tungsten Arc Welding (GTAW) technique is preferable over the cheaper and lower production rate Shielded Metal Arc Welding (SMAW) process. A good option that combines the quality performance of the GTAW process with the cheapness of the SMAW process is to make a first root pass using the GTAW process and complete the weld using SMAW rods.

If the GTAW roots pass is applied using the same filler metal used for the SMAW passes, few differences are to be expected between them regarding microstructure and mechanical properties. This changes completely if a different filler material is used, perhaps due to urgency when no other suitable filler is available. In these cases, a change in the properties of the joint is almost sure. These changes could be positive or negative, but in any case they have to be studied and evaluated.

The objective of this study is to evaluate the changes in the characteristics of a ductile cast iron butt joint when a GTAW ERNiCrMo-3 (trade name Inconel-625®) root pass is put on before SMAW Ni weld cover passes and to compare them with the characteristics of a fill SMAW joint when the filler metal is a high purity Ni alloy. This will be done in two circumstances: before and after an annealing post-treatment to dissolve any hard precipitates and restore the microstructure of the heat affected zone.

2. EXPERIMENTAL PROCEDURES

2.1. Materials

The chemical composition and mechanical properties of the ductile iron used in this study are shown in Table 1 and Table 2.

Sample plates were produced by sand casting process and originally sized to 300×95×11 mm (18.81×3.74×0.43 in). They were subsequently machined to 300×95×10 mm (18.81×3.74×0.39 in)

TABLE 1. Alloying elements of the ductile cast iron (wt.%).

C	Si	Mn	S	P	Ni	Cu	Cr	Mg	Fe
3.71	2.54	0.04	<0.01	0.02	0.02	0.026	0.03	0.03	rest

TABLE 2. Mechanical properties of the ductile cast iron base metal.

Tensile strength, R_M (MPa)	370	Break strain, A_B (%)	6
Yield strength, R_Y (MPa)	320	Hardness (HV)	160

to obtain coupons. The edges were prepared for welding with a single 30° bevel so that with proper spacing a perfect union could be achieved along the entire thickness of both plates. No relevant distortions were present in the test plates.

2.2. Welding

The electrodes used for welding were selected to obtain optimum results in terms of the mechanical properties and post-process of castings joining. The composition of the main filler material was 97.6% Ni, metal that minimizes carbide formation as well as improves service performance. The composition of the ERNiCrMo-3 wire used for the root passes can be seen in Table 3.

Four coupons were welded using two different processes. Half of them were welded using the shielded metal arc welding (SMAW) process, one of the most used for welding ductile cast iron, with 97.6% Ni coated electrodes. For the other half of the coupons, a root pass was put in using the gas tungsten arc welding (GTAW) process and ERNiCrMo-3 wire. Two cover passes with 97.6% Ni electrodes using the SMAW process completed the weld bead.

GTAW root welding using 1.5 mm (0.06 in) diameter ERNiCrMo-3 source material was carried out using a continuous welding current between 120–130 A, 22 V of direct polarity, and 12 $l \cdot min^{-1}$ of argon flow. The root weld was made in a single pass with a horizontal right to left motion. The tungsten electrode was inclined between 70° and 80° when moving forward and about 20° above horizontal for the source rod.

The SMAW welds were performed with direct current and reverse polarity due to the basic character of the coating, applying 140 A to 3.2 mm diameter electrodes that were previously heated for 24 h at 100 °C (212 °F) to improve fluidity and prevent cracking by hydrogen. Welds were carried out with horizontally, with two cover passes from left to right, and an electrode inclination angle of 60°. The weld passes were made in lengths of approximately 40 mm that were peened while hot with a small peen hammer to relieve cooling strains.

Due to the difficulty in welding cast irons all the coupons were preheated to 350 °C (662 °F) before welding in order to reduce stresses, slow the cooling rate, and increase the fluidity of the welds. That prevents pores forming and cracks in the bead and facilitates working with a minimum electrical current. A suitable separation of 2 mm between coupons was made to prevent undercuts and ensure a good penetration.

Other problems that can arise when welding cast irons are related to the breakdown of the electrodes coating, an excessive intensity as the weld progress or a lack of fluidity. It was decided to change the electrodes when one-half was consumed and so avoid deterioration by decomposition, thereby preventing porosity formation or internal inclusions. The electrodes were reused once cold. Due to the heating of the material, less and less current was required, but the intensity could not be reduced in excess because then electrode sticking could take place. Changing the electrode before it was consumed provided sufficient cooling time for the material without having to reduce intensity. Moreover, it was possible to vary the speed of the welding movement to prevent the filler source rod deterioration.

2.3. Heat post-treatments

Once the welds were finished, half of the joints were air-cooled while the other half were immediately annealed at 900 °C for 1 h to dissolve any possible martensitic structures and carbides that may appear as a consequence of the rapid cooling experienced under normal conditions when welding is stopped, despite using Ni.

These last samples were subsequently cooled in the furnace. This means the joints can be divided in four groups:

- Group 1: Without GTAW ERNiCrMo-3 root pass and without post-treatment
- Group 2: Without GTAW ERNiCrMo-3 root pass and with post-treatment
- Group 3: With GTAW ERNiCrMo-3 root pass and without post-treatment
- Group 4: With GTAW ERNiCrMo-3 root pass and with post-treatment

TABLE 3. Chemical composition of the filler materials used in the study (wt.%).

Filler	Ni	Cr	Mo	Ta	Nb	Si	Mn	C	Fe
ERNiCrMo-3	58	20–25	8–10	4.5	3.5	0.5	0.5	<0.1	rest
Ni-electrode	97.6	-	-	-	-	0.4	0.2	<0.1	rest

2.4. Results evaluation

Vickers microhardness (HV) was measured at the weld bead (WB), the interface between that zone and the heat affected zone (HAZ), and at the HAZ. Figure 1 shows the location of these zones at the joint. Results were obtained maintaining a load of 300 g during 10 s in nine different points. Tensile tests to determine the mechanical properties were carried out with an Instron universal testing machine at room temperature in accordance with UNE-EN ISO 6892-1. The measured mechanical properties were yield strength (R_Y), ultimate strength (R_M) and elongation at fracture (A_B). Figure 2 shows the main dimensions of the tensile test samples and where they were cut.

Metallographic examination of joints was carried out by means of a Nikon Microphot FX optical microscope after cutting and preparing the samples using standard procedures. Nital 5 was used to reveal the microstructure of the joints. An EDX (Energy-dispersive X-ray spectroscopy) composition analysis was carried out with a Jeol electronic microscope.

3. RESULTS

Figure 3 shows a welded coupon when a root ERNiCrMo-3 is put before completing the weld with a Ni electrode. The original geometry of the welded plates is also presented in the figure. Other coupons show a similar aspect. For reference, the various zones of the weld named in this chapter can be seen in.

The mechanical properties of the various tested samples are resumed in Table 4 (hardness) and 5 (strength). No appreciable difference has been found for the hardness values of the SMAW 97% Ni passes between groups 1 and 3 or between groups 2 and 4 due to the fact that their composition and thermal treatment have been the same.

The microstructure of the HAZ for samples belonging to groups 1 and 3 (before the annealing) is characterized by a mixture of martensite, bainite, perlite, graphite nodules and areas of ferrite around the graphite, although these areas are not always present near the interface. The presence of hard constituents diminishes as the distance to the interface increases. According to Table 4, the hardening at the HAZ without heat post-treatment, regardless of the welding technique and the filling material, has a mean value slightly over 300 HV near the interface, although actually this value varies from a maximum next to the interface to the original hardness of the cast iron at the edge of the HAZ, where the transformations induced by the heat input and the subsequent cooling disappear. After the annealing (samples of groups 2 and 4) the microstructure at the HAZ changes to a more stable one, with graphite nodules in a ferritic matrix, and the hardness at the HAZ falls to, approximately, 160 HV. The observed differences in hardness values at the HAZ for GTAW and SMAW passes are supposed to be simply effect of statistical dispersion when measuring over an area with variable hardness values. The microstructure of the HAZ before and after the annealing can be seen in Figs. 6 and 7.

The chemical composition of the weld bead and, thus, its microstructure, depends not only of the cooling speed, but also on the dilution, which is defined as the amount of base material that is fused and mixed with the filler material. This process has as a result a metal with a composition and properties that

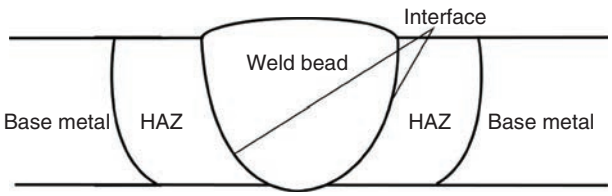

FIGURE 1. Image of the different zones in a weld: Weld bead (fused material), heat affected zone (HAZ) and base metal not affected by heat.

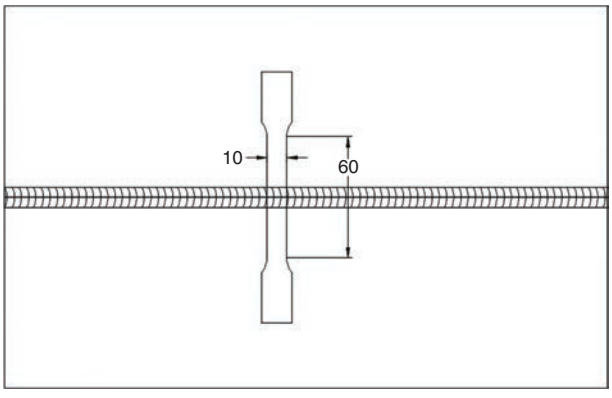

FIGURE 2. Welded plates and placement and main dimensions of the tensile test samples (only one sample is shown).

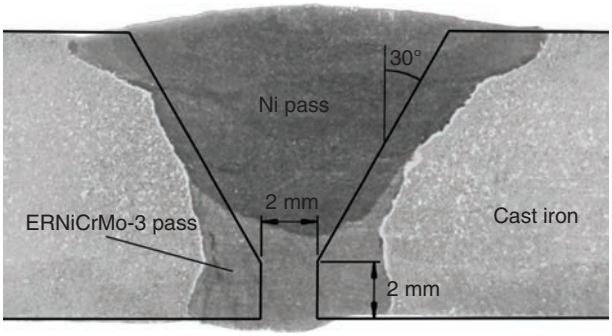

FIGURE 3. Macrography of a welded coupon attacked with Nital-3 superposed with the original geometry of the plates. These images were used to obtain dilution values.

TABLE 4. Hardness values at the HAZ, the weld bead and the interface band. Values for SMAW 97% Ni passes were the same for groups 1 and 3 and for groups 2 and 4. The main constituents of the zone are also shown.

	HAZ	Interface	Weld bead
SMAW 97% Ni (Groups 1 and 3)	320.5 near the interface (martensite/bainite)	391.0 (martensite) 762.9 (ledeburite)	172.9 (γNi)
Annealed SMAW 97% Ni (Groups 2 and 4)	157.1 (ferrite)	497.8 (martensite)	166.8 (γNi)
GTAW ERNiCrMo-3 (Group 3)	312.6 near the interface (martensite/bainite)	423.5 (martensite/bainite and carbides)	458.1 (centre – Fe-Ni-Cr and lamellar carbides) 765.7 (sides – Ni hard cast iron)
Annealed GTAW ERNiCrMo-3 (Group 4)	160.3 (ferrite)	207.4 (ferrite and some carbides)	539.4 (centre – Fe-Ni-Cr, lamellar carbides and fine precipitates)

differs from both the cast iron and the filler metal. For the SMAW passes dilution can be estimated to be about 30%. When Ni is used as filler material, its hardness has a mean value of 172.9 HV in the unannealed condition and 166.8 HV after the annealing. This minimum difference in the hardness values evidences the absence of metallurgical changes during the heat treatment at the 97% Ni passes, which is something expected due to the austenitic nature of the weld bead.

Hardness at the root passes when they are made using ERNiCrMo-3 shows a very different behaviour and properties. Furthermore, their characteristics are controlled by the fact that dilution had a very high value of about 75%, which means that the root pass has Fe as its main alloy element and only a small percentage of ERNiCrMo-3 enters in the composition. Another important fact is that the composition varies substantially along the different areas of a transversal cut of the root pass. The center of the root pass for group 3 samples (Fig. 4a) is composed by an austenitic matrix of, approximately: 76.5% Fe, 8% Cr and 7% Ni in weight, with other amounts of Mo or Mn. A dark lamellar intergranular phase shows a greater richness in C, Cr, and, also, Mn forming, possibly, carbides (Zhang *et al.*, 1995). This confers it a higher hardness.

At this zone and before the annealing (group 3 samples) hardness reaches 458 HV and after the heat treatment (group 4), the measured hardness goes up to 539.4 HV. This hardening is due to the massive precipitation of intergranular hardening particles, which can be seen in Fig. 4b as dispersed dark dots inside the grains. The exact nature of these precipitates remains to be studied. As the distance to the center of the of the ERNiCrMo-3 root increases and we approach the interface with the HAZ, the microstructure changes in this area and is substituted by a more complex one close to the interface with the base metal, as can be seen in Fig. 5a. This microstructure is composed by different phases, although Fe is again the main alloy element with percentages that varies between 64 and 85% in weight. Lighter zones have the same composition than the matrix of figure 4a; browner zones have a higher content in Cr, which can represent up to a 20% in weight; while the darkest areas shows a higher content in C and Si (up to 2.5%) but less than 2.3% Cr. The mean composition of the weld bead in this area resembles that of a Ni-Hard white cast iron. The high hardness of these zones, greater than 750HV seems to confirm the existence of this kind of hard cast iron in the weld bead at the root pass, with carbides and a Fe-Cr-Ni austenitic matrix with fine carbides.

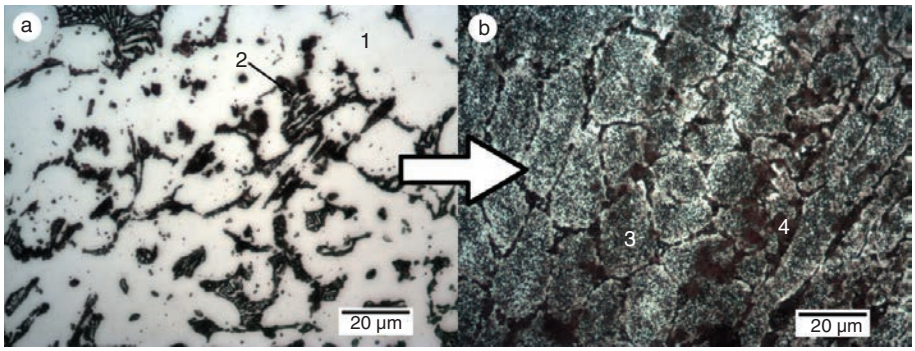

FIGURE 4. Microstructure at the center of the GTAW ERNiCrMo-3 root pass before (a) and after (b) an annealing at 900 °C. 1: Fe-Ni-Cr austenitic matrix; 2: eutectic carbides; 3: Small carbide precipitates in an Fe-Ni-Cr austenitic matrix; 4: eutectic carbides.

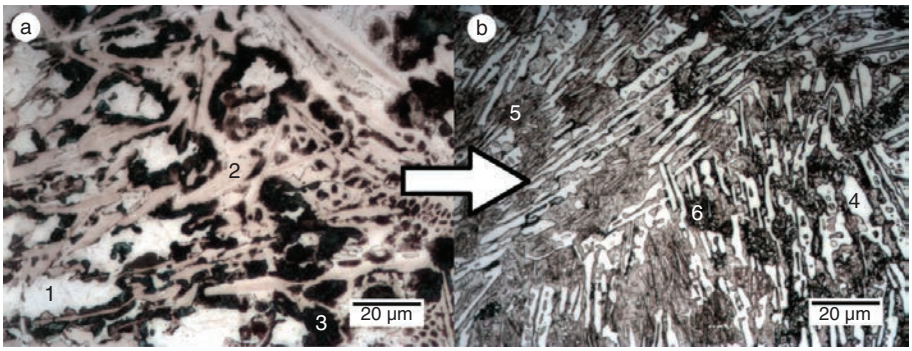

FIGURE 5. Microstructure near the interface with the base metal of the GTAW ERNiCrMo-3 root pass before (a) and after (b) an annealing at 900 °C. 1: Fe-Ni-Cr austenitic matrix; 2 and 3: carbides; 4: carbides; 5 and 6: Fe-Ni-Cr austenitic matrix with fine carbides.

After the annealing (Fig. 5b), two phases are visible near the interface. The one that forms a matrix with fine carbides has, according to an energy-dispersive X-ray spectroscopy (EDS) analysis, a composition of: 84% Fe, 3.5% Si, 2% Cr, 0.4% Mn, 4% Ni in weight, while the white phase (carbides) does not have Si in its composition and only a 0.65% of Ni, although its Cr content reaches 10%. In this case the harness of the annealed samples falls to 539.4 HV.

Figure 6 shows the microstructure at the HAZ, the interface and the base material for Ni SMAW passes before (group 1) and after the annealing post-treatment at 900 °C (group 2).

The interface at the Ni SMAW passes before the annealing treatment (group 1) is characterized by the presence of the eutectic ledeburite along it (Zhang *et al.*, 1996). This brittle and hard phase (up to 726.9HV) is surrounded by lath martensite (~400HV), creating an easy path for cracks to grow. This microstructure implies that part of the base material at the interface was melted and transformed to ledeburite during the posterior solidification, but the other part was only austenized because of the lower temperature it reached, and during the fast cooling phase it was transformed to martensite/bainite. The existence of ledeburite requires a high carbon content that comes from the original perlitic-ferritic matrix of the cast alloy.

The annealing of the samples leads to the dissolution of the ledeburite phase at the interface and to the transformation of the hardened microstructure of the HAZ to ferrite. Nevertheless, the stable structures are not fully recovered and a band of tempered martensite, with a hardness of 497.8 HV, remains at the interface, as can be seen in Fig. 6b. This proves that 1 hour of thermal treatment is not enough to eliminate every hardened structures.

Figure 7 show the microstructure at the interface for the ERNiCrMo-3 root passes before (group 3) and after the annealing post-treatment at 900 °C (group 4). The characteristics of the interface at the SMAW passes are the same described for groups 1 and 2 previously. So, only the microstructure at the root passes remains to be studied.

At the partial fusion zone of the GTAW root passes the presence of ledeburite phase becomes scarce and appears mixed with fine carbide precipitates instead of martensite. The hardness at the interface reaches more than 420 HV, which is considerably less than the hardness of the ledeburite that appears

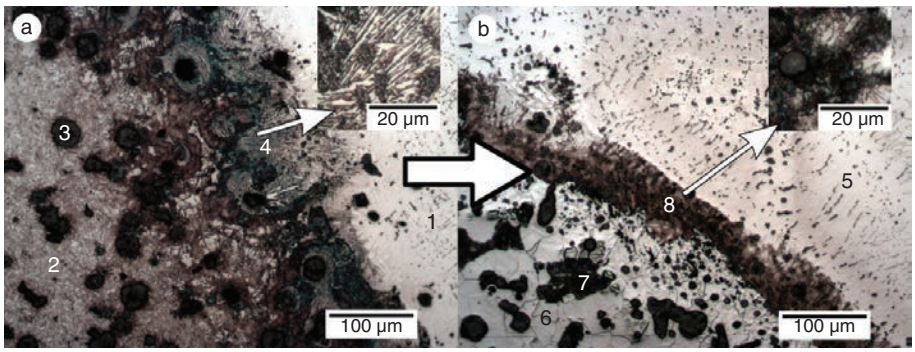

FIGURE 6. Microstructure of the interface with the base metal for the 97.6% Ni SMAW passes before (a) and after (b) an annealing at 900 °C. 1:Ni alloy; 2: martensite/bainite; 3: graphite nodules 4: ledeburite; 5: Ni alloy; 6: Ferrite; 7: graphite nodules; 8: tempered martensite

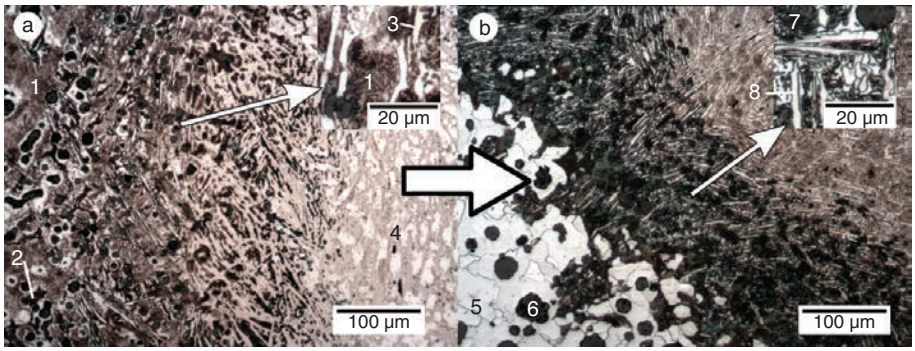

FIGURE 7. Microstructure of the interface with the base metal for the GTAW ERNiCrMo-3 root passes before (a) and after (b) an annealing at 900 °C. 1: martensite/bainite; 2: graphite nodules; 3: carbides; 4: Ni-Fe-Cr alloy; 5: ferrite; 6: graphite nodules; 7: Fe-Ni-Cr austenitic matrix with fine carbides; 8: carbides.

at the interface in the SMAW Ni passes. During the heat treatment, the small carbides precipitates are dissolved and a mixture of perlite, ferrite, graphite nodules and a Cr-enriched and Si-free phase forms the microstructure. This structure is softer and gives a hardness of only 207 HV.

The mechanical properties of the joints (Table 5) show differences depending on the filler material and the annealing post-treatment. When compared to the properties of the original nodular cast iron (Table 2) all the tested samples show a decrease in the values of ultimate and yield strength. Group 1 samples have, despite the presence of ledeburite at the interface zone, the higher mechanical strength of all the joints (RY=340 MPa and Y=335 MPa) due to the use of Ni-based consumables, which reduce both metal shrinkage and thermal stress during solidification, leading to a reduction of cracking susceptibility. Another benefit is that it improves the tolerance to phosphorus and sulphur and reduces the risk of hot cracking (Pouranvari, 2010). This loss of strength when compared to the base metal is accompanied by a notable increase in elongation at break that goes from 6% up to 14%. After the annealing (group 2) the mechanical properties suffer a further decrease, not very important for the ultimate or yield strength, but elongation goes down to values around 8%, still higher than the original 6%. It can be concluded that the remaining martensite at the weld interface seems to have a more pernicious effect than the existence of a harder ledeburite phase.

The ultimate and yield strengths of group 3 samples (with ERNiCrMo-3 root pass) show similar values to the ones measured for group 2 samples, although with a lower elongation. This elongation of 5.5% falls below the elongation of the cast iron, what implies a total low of properties, both in resistance and ductility. After the annealing (group 4) the mechanical resistance of the joint continues to fall and ductility recovers, with values of 7% for elongation, slightly over the elongation of the base cast iron. This recovery is supposed to be related to the decrease of maximum hardness at the weld root pass, while the further loss of mechanical properties could be related to the mean hardness value over the root pass section.

TABLE 5. Mechanical properties of the tested samples

	Group 1	Group 2	Group 3	Group 4
R_M (MPa)	340	320	320	300
R_Y (MPa)	335	310	310	285
A_B (%)	14	8	5.5	7

4. DISCUSSION

The study of the microstructure of the joints shows that the presence of a GTAW root pass, despite the low percentage of the total volume it represents, can change notably the properties of the weld if a different source metal is used. In this case, the source material for the root pass was ERNiCrMo-3, which is a Ni-Cr alloy, and thus, will add a high Cr content to the weld bead in comparison with the SMAW Ni passes, where no Cr can be found. Another difference between the GTAW root pass and the SMAW cover passes was the high dilution associated with the first one. This fact implies that the composition of the bead at the root is extremely different from that of the source material and a lot more similar to the cast iron.

When the samples of nodular cast iron are welded using the SMAW technique and Ni electrodes, the austenitic Ni weld bead provides a deformable volume of material that increases elongation at break up to values that double the original ones of the cast iron. Although a decrease in ultimate and yield strength is to be expected, the global characteristics of the joint can be considered acceptable. A layer of hard and fragile ledeburite appears at the interface of the welded metal with the HAZ (Fig. 6a), but its influence seems to be balanced by the Ni bead.

After an annealing treatment a recovery of characteristics is supposed to accompany the recovery of a more stable microstructure. However, after the heat treatment and despite no traces of ledeburite could be found, a band of martensite remained at the interface (Fig. 6b). The presence of this martensite is a consequence of the insufficient annealing time, which should be increased to obtain a total dilution of hard structures. In this case, a slight decrease in mechanical strength and a higher loss of elongation was observed, although elongation was still higher than the elongation associated with the nodular cast iron.

When an ERNiCrMo-3 root pass is put on before the cover passes the different composition of this pass and the high dilution lead to the formation of hard structures during solidification. Furthermore, the microstructure of the root pass is different at its centre and near the interface. At the centre, an austenitic matrix is accompanied by a harder intergranular phase that could be identified as carbides. Near the interface with the HAZ the root pass show the aspect and chemical composition of a Ni-hard white cast iron, with a hardness of 750 HV. Evidently, the root pass has more fragile behaviour than the cover Ni passes and is unable to follow the Ni cover passes in their deformation during the tensile test. Although no further loss of ultimate strength was detected, elongation at break was substantially reduced below the original values of the cast iron, what supposes an inadmissible decrement in the joint characteristics.

An annealing at 900 °C of 1 h fails again to provide a soft metallurgical microstructure in the totality of the joint. Although the hard structures of the HAZ and the interfaces disappear, the hardness at the root pass remains high and even increases due to a precipitation of hard particles at its centre zone. The yield and ultimate strength of the joint is the lower of all samples but an improvement in elongation is achieved.

All these results show that the use of a root ERNiCrMo-3 pass can improve penetration but, at least at high dilutions, at the cost of an important loss of mechanical properties, both strength and elongation. Under these circumstances is preferable to avoid the root pass and use a full Ni SMAW process.

5. CONCLUSIONS

- A GTAW ERNiCrMo-3 root pass with a high dilution value leads to a very hard microstructure after cooling. Hardness reaches its higher values near the interface with the HAZ.
- The presence of a hard and brittle root pass implies a reduction in ductility and mechanical strength, independently of the behaviour of the cover passes. The characteristics of the resulting joint are worse than the ones of the base material or the obtained with a full SMAW Ni joint.
- An annealing post-treatment at 900 °C for 1 h was not enough to dissolve all hard structures in the full SMAW joint and a line of tempered martensite remained at the interface, what caused a slight loss of properties.
- Annealing of the joints with the ERNiCrMo-3 root passes did not lead to an improvement in ultimate or yield strength, although a slight recovery of ductility was detected.
- In terms of toughness, ductility, tensile and yield strength, ductile cast iron coupons welded exclusively with Ni electrode by the SMAW technique performed better than those made with ERNiCrMo-3 root welding GTAW and followed by Ni-SMAW passes. An annealing heat treatment did not change these conclusions.

REFERENCES

Arabi Jeshvaghani, R., Jaberzadeh, M., Zohdi, H., Shamanian, M. (2014). Microstructural study and wear behavior of ductile iron surface alloyed by inconel 617. *Mater. Design* 54, 491–497. http://dx.doi.org/10.1016/j.matdes.2013.08.059.

Castolin (1993). *Eutectic Castolin: Practice Handbook* (Spanish Edition). Ed. Castolin España, SA Madrid, pp. 64. https://www.castolin.com/es-ES/publications.

Cembrero, J., Pascual, M. (1999). Soldabilidad de las fundiciones de grafito esferoidal. *Rev. Metal.* 35 (6), 392–401. http://dx.doi.org/10.3989/revmetalm.1999.v35.i6.648.

El-Banna, E. (1999). Effect of preheat on welding of ductile cast iron. *Mater. Lett.* 41 (1), 20–26. https://doi.org/10.1016/S0167-577X(99)00098-1.

El-Banna, E.M., Nageda, M.S., El-Saadat, M.A. (2000). Study of restoration by welding of pearlitic ductile cast iron. *Mater. Lett.* 42 (5), 311–320. https://doi.org/10.1016/S0167-577X(99)00204-9.

Huke, E.E., Udin, H. (1953). Welding metallurgy of nodular cast iron. *Weld. J.* 32 (8), 378s–385s.

Kiser, D., Faws, P.E., Northey, M. (2005). Welding Cast Iron. Fall 2005, Canadian Welding Association Journal, pp. 1–4. http://selector.specialmetalswelding.com/publica/cwa-fall2005.pdf.

Martínez, R.A., Sikora, J.A. (1995). Pearlitic Nodular Cast Iron: Can It Be Welded?. *Weld. J.* 74 (3), 63–73.

Pascual, M., Cembrero, J., Salas, F., Pascual Martínez, M. (2008). Analysis of the weldability of ductile iron. *Mater. Lett.* 62 (8-9), 1359–1362. https://doi.org/10.1016/j.matlet.2007.08.070.

Pease, G.R. (1960). The Welding of Ductile Iron. *Weld. J.* 39 (1), 1–9.

Pouranvari, M. (2010). On the weldability of grey cast iron using nickel based filler metal. *Mater. Design* 31 (7), 3253–3258. https://doi.org/10.1016/j.matdes.2010.02.034.

Zhang, X.Y., Zhou, Z.F., Xie, M.L., Zhang, Y.M. (1995). A Newly Developed Nickel-Iron Electrode with Superior Hot Cracking Resistance and High-Strength Properties for Welding Perlitic Nodular Iron. *Welding Research Supplement* 1, 16–20. https://app.aws.org/wj/supplement/WJ_1995_01_s16.pdf.

Zhang, X.Y., Zhou, Z.F., Zhang, Y.M., Wu, S.L., Guan, L.Y. (1996). Influence of Nickel-Iron Electrode Properties and Joint Shapes on Welded Joint Strength of Pearlitic Nodular Iron. *Welding Research Supplement* 9, 280–284. https://app.aws.org/wj/supplement/WJ_1996_09_s280.pdf.